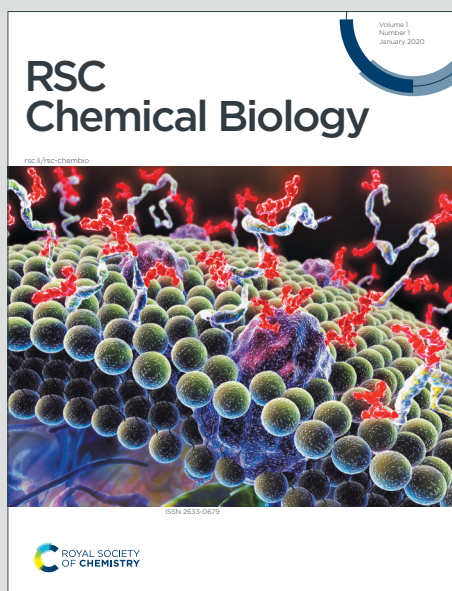


# RSC Chemical Biology

Accepted Manuscript

This article can be cited before page numbers have been issued, to do this please use: J. Bai, F. Guo, M. Li, Y. Li and X. Lei, *RSC Chem. Biol.*, 2021, DOI: 10.1039/D1CB00002K.



This is an Accepted Manuscript, which has been through the Royal Society of Chemistry peer review process and has been accepted for publication.

Accepted Manuscripts are published online shortly after acceptance, before technical editing, formatting and proof reading. Using this free service, authors can make their results available to the community, in citable form, before we publish the edited article. We will replace this Accepted Manuscript with the edited and formatted Advance Article as soon as it is available.

You can find more information about Accepted Manuscripts in the [Information for Authors](#).

Please note that technical editing may introduce minor changes to the text and/or graphics, which may alter content. The journal's standard [Terms & Conditions](#) and the [Ethical guidelines](#) still apply. In no event shall the Royal Society of Chemistry be held responsible for any errors or omissions in this Accepted Manuscript or any consequences arising from the use of any information it contains.

## ARTICLE

**Click-based amplification: designed to facilitate various target labelling with ultralow background**Jinyi Bai<sup>ab</sup>, Fusheng Guo<sup>ab</sup>, Mengyao Li<sup>c</sup>, Yulong Li<sup>\*bc</sup> and Xiaoguang Lei<sup>\*ab</sup>Received 00th January 20xx,  
Accepted 00th January 20xx

DOI: 10.1039/x0xx00000x

We here describe a fluorescent signal amplification method termed as “Click-based amplification” that can be well integrated with various click-labelling modes, including chemical labelling, genetic incorporation and covalent inhibitor probe mediated target labelling. Picolyl azide (pAz) was used as a functional group of amplifier to enhance the efficiency of click chemistry. Click-based amplification provided 3.0-12.7 fold amplification on fixed HeLa cells with different click-labelling modes. Click-based amplification has proven to be superior to tyramide signal amplification (TSA) in view of the nonspecific amplification and the signal-to-noise ratio. Moreover, in terms of the challenging signal amplification of tissue specimen, Click-based amplification successfully achieved remarkable fluorescence enhancement on intestinal tissue slices of Afatinib-N<sub>3</sub> treated mice, which provided direct evidences of the existence of Afatinib-N<sub>3</sub> in intestinal tissues and helped to reveal the off-target toxicity of afatinib. Collectively, these results illustrate that Click-based amplification would serve as a promising method for bioimaging studies.

**Introduction**

Signal amplification is widely demanded in various applications including western blotting, ELISA, microscopy and clinical diagnosis. Different signal amplification strategies have been developed to meet various requirements in practical applications. Tyramide signal amplification (TSA) uses horseradish peroxidase (HRP) conjugated streptavidin and antibodies as reporters to amplify signals by catalysing labelled tyramide substrates deposition.<sup>1</sup> Hybridization chain reaction (HCR) utilizes one initiator DNA strand to trigger a cascade of hybridization events of two stable species of DNA hairpins, providing a linear amplification.<sup>2</sup> Furthermore, to combine hybridization-based signal amplification methods with antibody-based immunostaining, immunosignal hybridization chain reaction (isHCR)<sup>3</sup> and immunostaining with signal amplification by exchange reaction (Immuno-SABER)<sup>4</sup> were developed and successfully used to amplify protein targets in tissues.

On the other hand, the abundance levels of biomolecules vary greatly. For example, the abundance of proteins in mammalian cells varies by at least seven orders of magnitude (about 10<sup>1</sup> to 10<sup>8</sup> copies per cell).<sup>5</sup> To amplify targets with a wider range of abundance, some controllable amplification methods are developed using stepwise amplification strategies. Click-amplifying FISH (clampFISH) is a signal amplification method using iterative rounds of hybridization and click-locking to amplify RNA and DNA targets with high specificity and high amplification efficiency.<sup>6</sup> Fluorescent signal amplification via cyclic staining of target molecules (FRACTAL) can amplify the signal intensity of immunofluorescence staining more than nine-fold via simple cyclic staining of secondary antibodies.<sup>7</sup> Multi-cycle amplification provides a successive growth of signal intensity, but the background amplification and the signal-to-noise ratio should be carefully examined during the amplification process. More importantly, most of current amplification methods share the same idea that target recognition depends on primary antibodies and hybridization reactions, resulting in the target range is limited to proteins and nucleic acids.

Non-proteinaceous biomolecules, including glycans and lipids also play important roles in various biology processes, but most of them show weak immunogenicity<sup>8</sup>. Chemical biologists have developed a click-labelling platform to visualize various biomolecules<sup>9-11</sup>: install unique functional groups into target molecules, then ligate visual tags and other reporters via bioorthogonal reactions. However, signal amplification methods tailored for click-labelling strategy are seriously inadequate. Carell and co-workers have reported a remarkable

<sup>a</sup> Beijing National Laboratory for Molecular Sciences, State Key Laboratory of Natural and Biomimetic Drugs, Key Laboratory of Bioorganic Chemistry and Molecular Engineering of Ministry of Education, Department of Chemical Biology, College of Chemistry and Molecular Engineering, Synthetic and Functional Biomolecules Center, Peking University, Beijing 100871, People's Republic of China

<sup>b</sup> Peking-Tsinghua Center for Life Science, Academy for Advanced Interdisciplinary Studies, Peking University, Beijing 100871, People's Republic of China

<sup>c</sup> State Key Laboratory of Membrane Biology, Peking University School of Life Sciences, Beijing, China; PKU-IDG/McGovern Institute for Brain Research, Beijing, China; Chinese Institute for Brain Research, Beijing, China

\* Correspondence Email: xglei@pku.edu.cn (X.L.); yulongli@pku.edu.cn (Y.L.)

Electronic Supplementary Information (ESI) available: [details of any supplementary information available should be included here]. See DOI: 10.1039/x0xx00000x



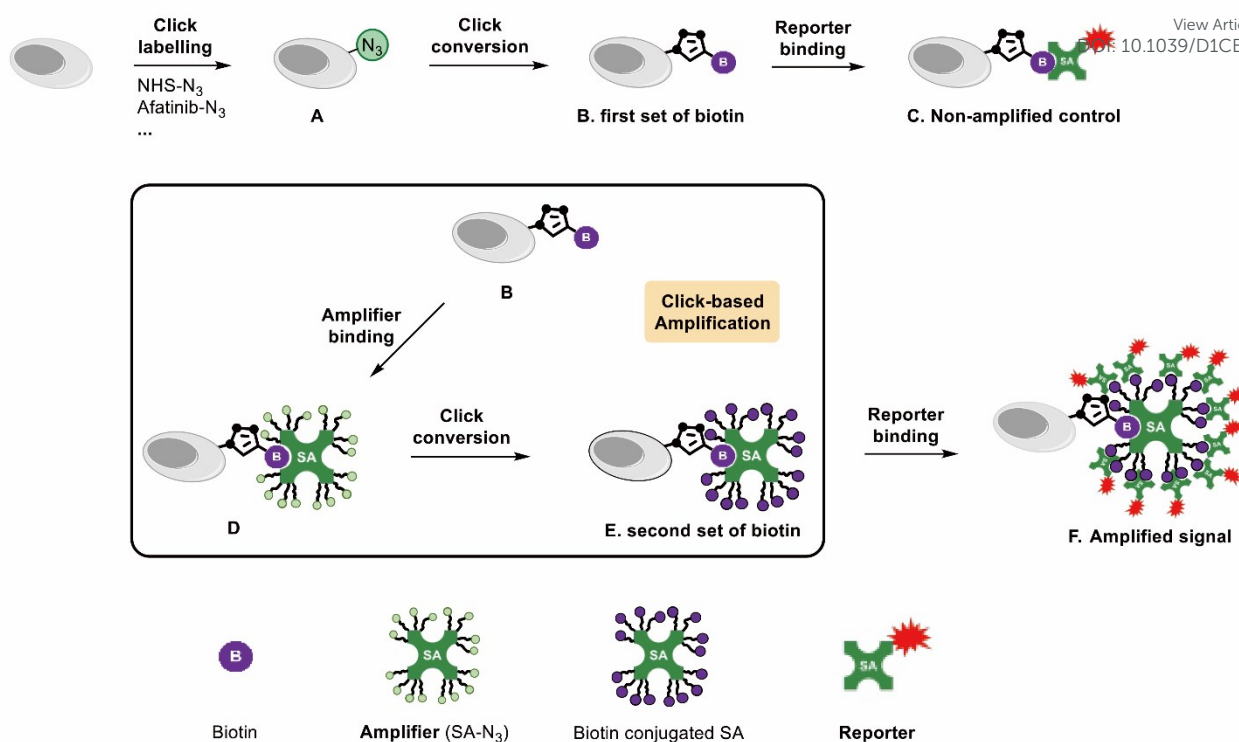


Fig. 1 Schematic representation of Click-based amplification procedure with streptavidin- $N_3$ . (A) Target of interest is labelled with azide. (B) The first set of biotin is introduced via click reaction. (C) Non-amplified control: streptavidin-AF647 binds to the biotin on target for imaging. (D) Amplifier binding step. Streptavidin- $N_3$  binds to the biotin on target and introduces multiple azide groups. (E) Click conversion step. A second set of biotin is introduced via click reaction. (F) Amplified signal: the additional biotin tags recruit more streptavidin-AF647 and gain enhanced fluorescence.

dendrimer-based signal amplification using click chemistry, and achieved fluorescence amplification for EdU-labelled DNA *in situ* with low background.<sup>12</sup> However, other click-labelling and more complex biological systems were not tested.

Herein, we report a signal amplification method, Click-based amplification that can amplify various click-labelling modes, including chemical labelling, genetic incorporation and covalent inhibitor probe mediated target labelling. Click-based amplification enhanced fluorescence signal of fixed HeLa cells by 3.0-12.7 fold without introducing obvious nonspecific amplification. Finally, Click-based amplification can be used to amplify the signal of mice intestinal tissue specimens, providing direct evidences of drug distribution in animal tissues.

## Results and discussion

### Click-based amplification design

The schematic representation of Click-based amplification in this study is shown in Fig. 1. The amplification procedure includes two steps: 1) amplifier binding, azide functionalized streptavidin (amplifier) binds to the biotin tag on target (Fig. 1D); 2) click conversion, a second set of biotin is introduced onto target via click reaction (Fig. 1E). The number of biotin tags on target will increase after this two-step amplification process (Fig. 1B and 1E), since there are 16 azide groups on the amplifier

in theory after saturated modification of streptavidin lysine residues with NHS- $N_3$ . Streptavidin is a tetramer protein, and every monomer contains 4 lysine residues: K80, K121, K132 and K134 (Fig. 2B, PDB: 3ry1)<sup>13</sup>. The saturated modification of the limited number of lysine residues can make a relatively homogenous amplifier and gain a moderate amplification efficiency. Multi-cycle amplification is feasible in design, and the procedure was shown in Fig. S1A. However, multi-cycle amplification may decrease the signal-to-noise ratio, since the amplified fluorescence of vehicle control may increase faster than that with click-labelling. Therefore, one cycle of amplification is recommended for the sake of signal-to-noise ratio and time cost.

### Optimization of Click-based amplification

**Choosing biotin-PEG<sub>4</sub>-alkyne as the click converter.** Click reaction was utilized to convert the azide groups on amplifier to biotin. Two types of widely-used click reactions are tested in Click-based amplification paradigm: copper(I)-catalyzed azide-alkyne cycloaddition (CuAAC)<sup>14</sup> and strain-promoted azide-alkyne cycloaddition (SPAAC)<sup>15</sup>. We carried out Click-based amplification with CuAAC-type converter biotin-PEG<sub>4</sub>-alkyne and SPAAC-type converter biotin-PEG<sub>2</sub>-DIBO in the context of fixed HeLa cells (Fig. S1A). The confocal imaging and fluorescence quantification results were shown in Fig. S1B and S1C. There was no significant increase of nonspecific



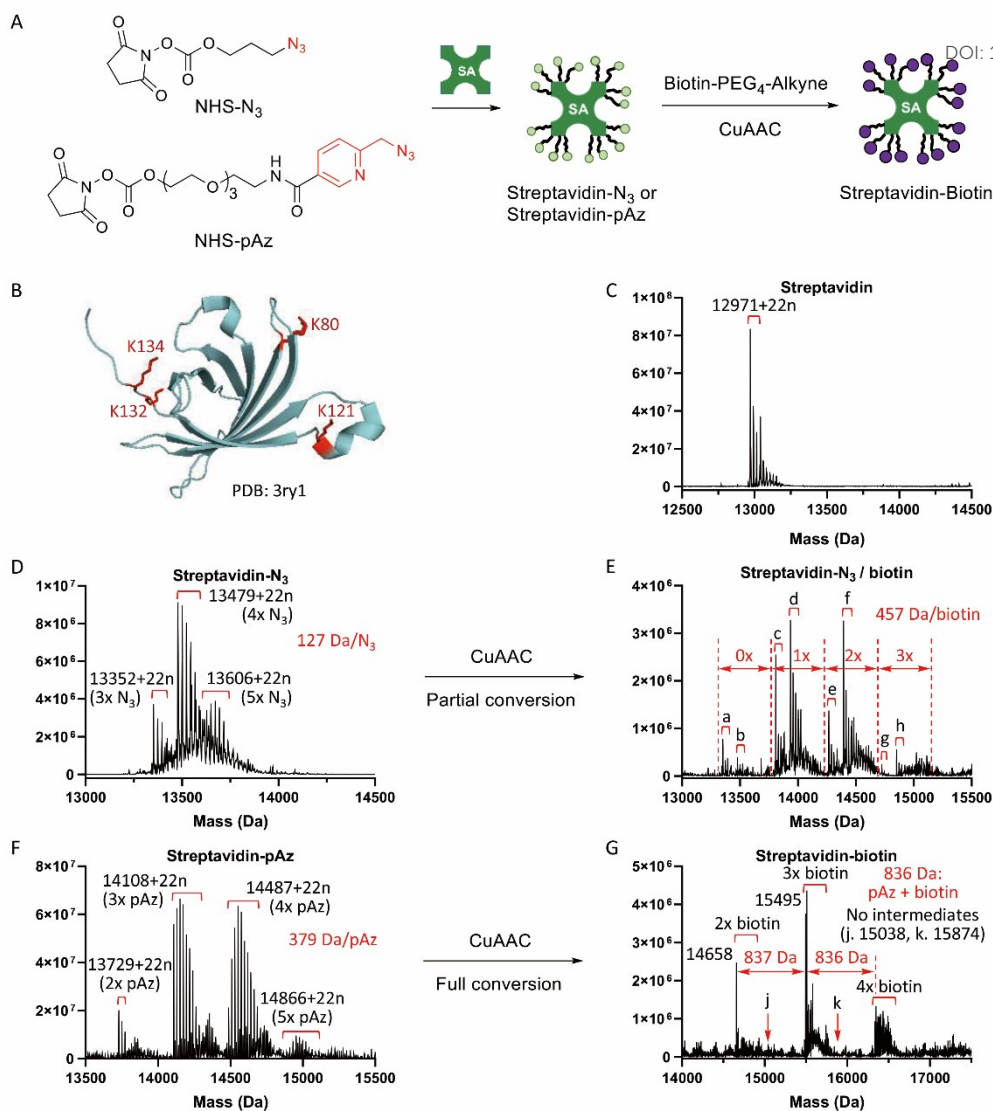


Fig. 2 Streptavidin-pAz showed much higher click conversion efficiency than streptavidin-N<sub>3</sub> in solution. (A) Reactions of two types of amplifiers synthesis and Click conversion. Streptavidin was modified with NHS-N<sub>3</sub> or NHS-pAz, generating two types of amplifiers streptavidin-N<sub>3</sub> and streptavidin-pAz. (B) Crystal structure of streptavidin monomer, including 4 lysine residues. (C) The deconvoluted ESI-TOF mass spectra of streptavidin monomer (mSA). Molecular weight (MW): 12971+22n.  $\Delta m = 22$  should be Na<sup>+</sup>. (D) Streptavidin modified with NHS-N<sub>3</sub>. The numbers of N<sub>3</sub> groups on streptavidin were calculated to be 3-5. (E) Partial conversion of streptavidin-N<sub>3</sub> in (D) via CuAAC with biotin-PEG<sub>4</sub>-alkyne. MWs of a-h: 13352+22n (3x N<sub>3</sub>, no biotin), 13479+22n (4x N<sub>3</sub>, no biotin), 13809+22n (2x N<sub>3</sub>, 1x biotin), 13936+22n (3x N<sub>3</sub>, 1x biotin), 14266+22n (1x N<sub>3</sub>, 2x biotin), 14393+22n (2x N<sub>3</sub>, 2x biotin), 14723+22n (no N<sub>3</sub>, 3x biotin), 14850+22n (1x N<sub>3</sub>, 3x biotin). (F) Streptavidin modified with NHS-pAz. The numbers of pAz groups on streptavidin were calculated to be 2-5. (G) Full conversion of streptavidin-pAz in (F) via CuAAC with biotin-PEG<sub>4</sub>-alkyne. MWs: 14658 (no pAz, 2x biotin), 15495 and 15509 (no pAz, 3x biotin), 16345 (no pAz, 4x biotin). No intermediates MWs: 15038 (1x pAz, 2x biotin), 15874 (1x pAz, 3x biotin).

fluorescence for biotin-PEG<sub>4</sub>-alkyne (Fig. S1C), while biotin-PEG<sub>2</sub>-DIBO introduced high nonspecific binding (Fig. S1D, No Amp., 1.8-fold) and high nonspecific amplification (Fig. S1D, 7.6-fold for Amp.x2, 8.7-fold for Amp.x4). DIBO was reported to show a relatively higher azide-independent labelling of proteins than terminal alkyne *in vitro*.<sup>16</sup> Hence the CuAAC-type converter biotin-PEG<sub>4</sub>-alkyne was chosen for Click-based amplification.

**Selection of picolyl azide (pAz) as a functional group of the streptavidin-based amplifier.** The number of azide groups on the amplifier and the efficiency of subsequent click conversion are

the key to gain signal amplification (Fig. 2A). We first quantified the number of azide groups on streptavidin after saturated modification with NHS-N<sub>3</sub> by ESI-TOF mass spectrometer, and the increased molecular weight showed that 3-5 azide groups were covalently linked on streptavidin monomer (Fig. 2D), indicating that a close-to-saturation modification of streptavidin was achieved, and that a small part of N-terminal  $\alpha$ -amine was also modified. However, there were only 1.53 biotin groups conjugated on streptavidin monomer after click reaction in solution (Fig. 2E, Fig. S2A). The low efficiency would reduce the overall amplification ratio. Picolyl azide (pAz) was found to accelerate the CuAAC reaction



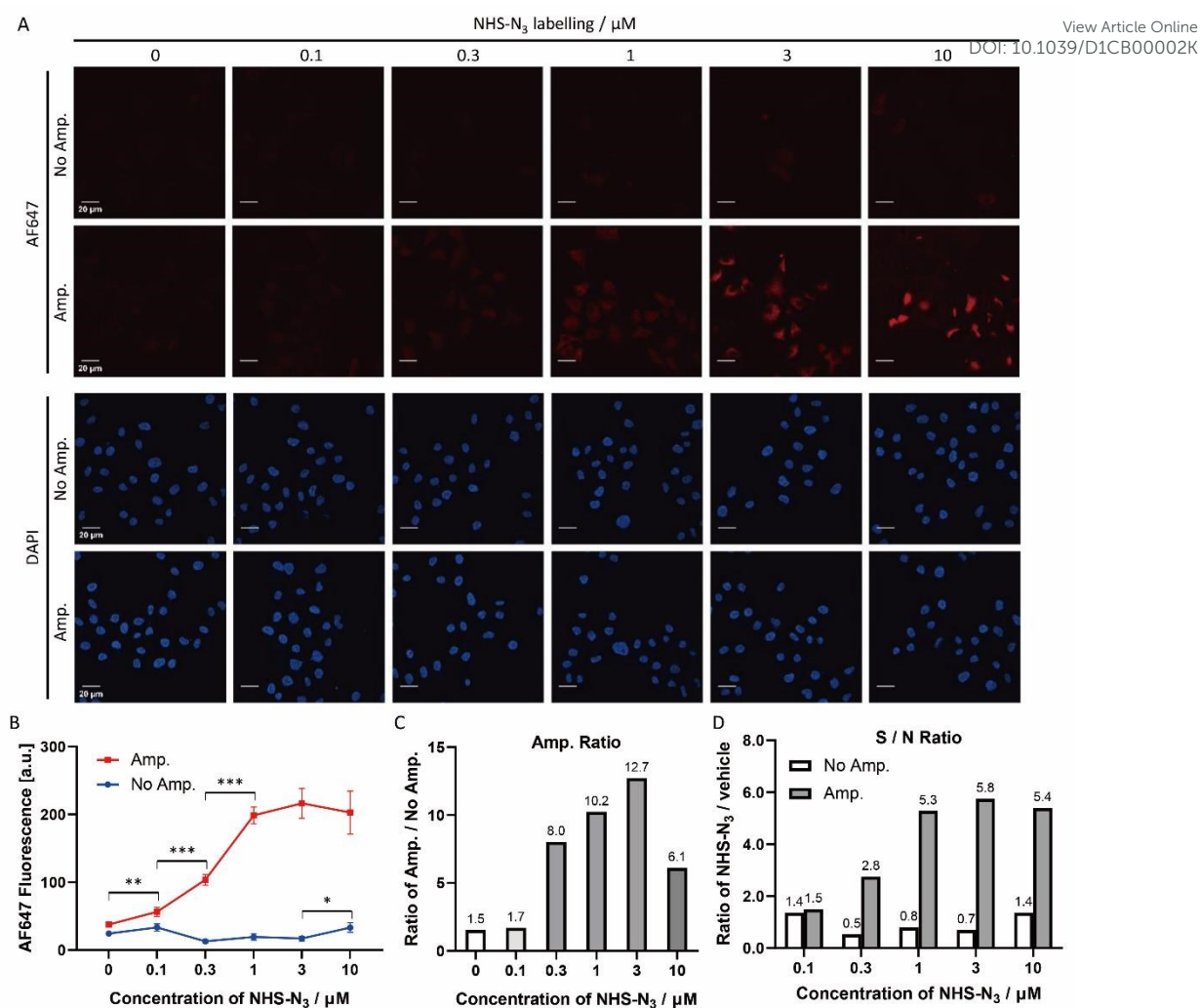


Fig. 3 Click-based amplification on fixed HeLa cells with NHS-N<sub>3</sub> labelling. (A) Confocal imaging of fixed HeLa cells without and with Click-based amplification (No Amp. and Amp.). HeLa cells were treated with a concentration gradient of NHS-N<sub>3</sub> from 0.1 μM to 10 μM. DAPI indicated the nucleus of the HeLa cell. Scale bar, 20 μm. (B) Quantification of cellular AF647 fluorescence intensity in (A) with ImageJ. Red line represents the fluorescence intensity of HeLa cells with Click-based amplification (Amp.), and each data point is the average fluorescence intensity of 20 cells chosen randomly from the microscope imaging. Blue line, the fluorescence intensity of HeLa cells without Click-based amplification (No Amp.). Error bar: the standard error (SE). (C) Amplification ratios (Amp. / No Amp.). (D) Signal-to-noise ratios (NHS-N<sub>3</sub> / vehicle). \*\*\* =  $p < 0.001$ , \*\* =  $p < 0.01$ , \* =  $p < 0.05$ .

more than ten-fold by the chelation effect with copper(I) catalyst.<sup>17, 18</sup> We then synthesized a new modification reagent NHS-pAz (Fig. S10), and carried out the saturated modification and click conversion using a same protocol. The results showed that 2-5 pAz groups were conjugated to streptavidin monomer (Fig. 2F), and the average number of pAz groups was 3.48 (Fig. S2B), comparable to the number of N<sub>3</sub> groups streptavidin-N<sub>3</sub> (Fig. 2D). But most importantly, all the pAz groups on streptavidin reacted with biotin-PEG<sub>4</sub>-alkyne in solution (Fig. 2G), and the average number of conjugated biotin groups was 3.16 (Fig. S2C). Hence the copper-chelating azide (pAz) was chosen for Click-based amplification.

#### Click-based amplification for NHS-N<sub>3</sub> labelling in HeLa cells

NHS-N<sub>3</sub> globally labelled the biomolecules containing primary amino groups in HeLa cell, i.e. proteins, lipids. To determine the suitable range of labelling concentrations for Click-based

amplification, HeLa cells were treated with a gradient of NHS-N<sub>3</sub> from 0.1 μM to 10 μM. The cellular AF647 fluorescence intensity of confocal imaging (Fig. 3A) was measured with ImageJ. In the amplification group (Fig. 3B, Amp.), HeLa cells treated with 0.1 μM of NHS-N<sub>3</sub> showed significantly increased cellular fluorescent signals comparing to vehicle group, while in the group without amplification (Fig. 3B, No Amp.), HeLa cells treated with 10 μM of NHS-N<sub>3</sub> began to show a labelling-dependent fluorescence enhancement. Click-based amplification therefore improved the detection sensitivity by at least 100-fold. To quantify the amplification efficiency, the amplification ratio was defined as the ratio of cellular fluorescence with Click-based amplification to that without amplification. Click-based amplification obtained fluorescence amplification by 6.1-12.7 fold in HeLa cells treated with 0.3-10 μM of NHS-N<sub>3</sub> (Fig. 3C). The signal-to-noise ratios of



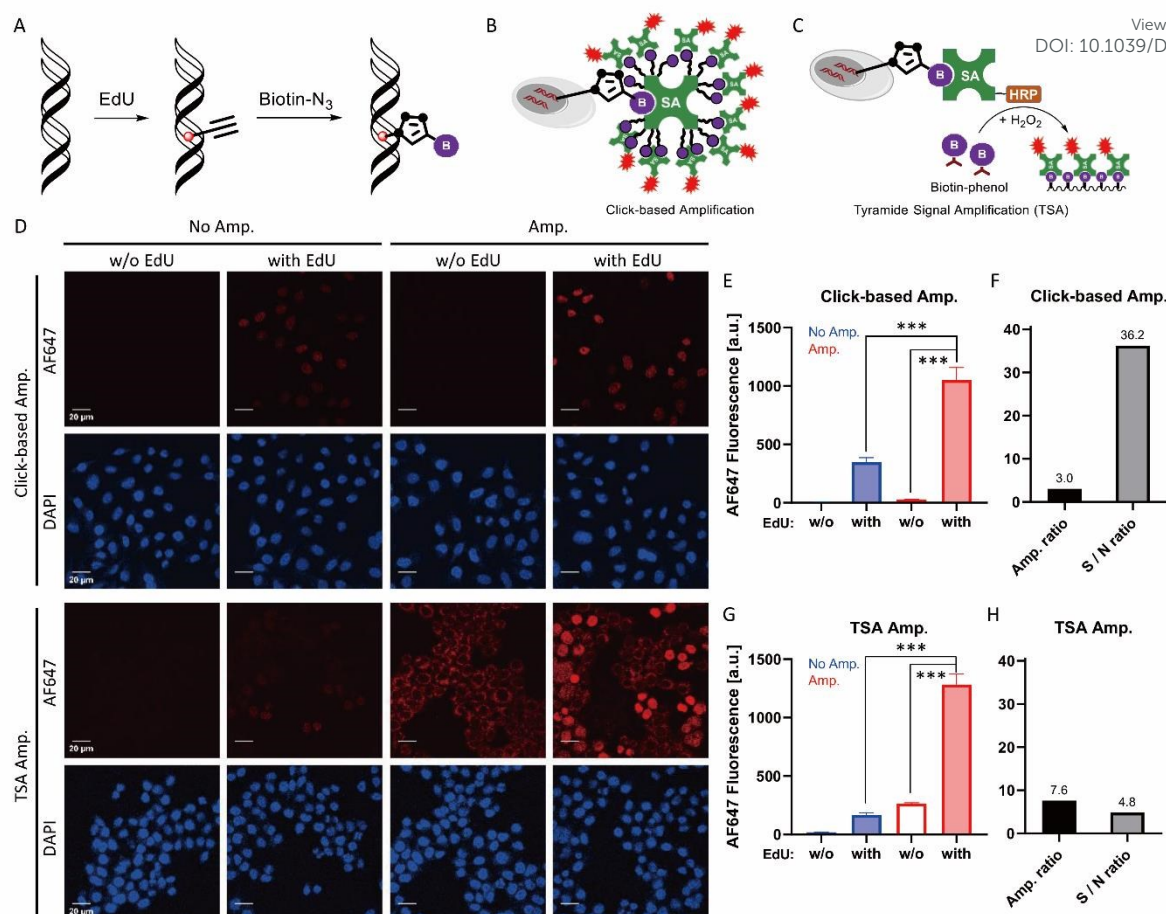


Fig. 4 Click-based amplification gained much higher signal-to-noise ratio than TSA on fixed HeLa cells with EdU labelling. (A) Scheme of DNA labelled with EdU and the click conversion of EdU to biotin. (B) Scheme of Click-based amplification. (C) Scheme of TSA. (D) Confocal imaging of fixed HeLa cells with Click-based amplification and TSA. HeLa cells were treated with 10 μM of EdU in DMEM at 37 °C for overnight. DAPI indicated the nucleus of the HeLa cell. Scale bar, 20 μm. (E) Quantification of cellular AF647 fluorescence intensity in (D) with Click-based amplification. For w/o EdU groups, all the cell nuclei were dark, and 20 cells were chosen randomly to average the fluorescence intensity. For with EdU groups, all the lighted nuclei were measured to average the fluorescence intensity. (F) Amplification ratio (Amp. / No Amp.) and signal-to-noise ratio (EdU / vehicle) with Click-based amplification. (G) Quantification of cellular AF647 fluorescence intensity in (D) with TSA amplification. For w/o EdU groups, 20 cells were chosen randomly to average the fluorescence intensity. For with EdU groups, all the lighted nuclei were measured to average the fluorescence intensity. (H) Amplification ratio (Amp. / No Amp.) and signal-to-noise ratio (EdU / vehicle) with TSA. \*\*\* =  $p < 0.001$ .

cellular fluorescence were also improved with Click-based amplification (Fig. 3D).

#### Click-based amplification for EdU labelling in HeLa cells

5-Ethynyl-2'-deoxyuridine (EdU) has been used to be genetically incorporated into DNA during cell division. This approach labels the newly synthesized DNA with alkyne group,<sup>10</sup> which can be converted to biotin tags via click reaction with biotin-N<sub>3</sub> (Fig. 4A). The nuclear positioning makes EdU labelling a suitable system to evaluate the fidelity of Click-based amplification. The confocal imaging results showed that Click-based amplification enhances the nuclear fluorescence signal but not cytoplasm (Fig. 4D). The amplification ratio of EdU labelling in HeLa cells was 3.0-fold (Fig. 4E and 4F). The relatively low amplification ratio may result from the highly crowded nuclear surroundings. To evaluate the potential application of Click-based amplification, we compared our results with the widely used tyramide signal amplification (TSA). TSA can be readily

integrated with various biotin labelling methods (Fig 4C). We performed TSA for EdU labelling in HeLa cells. The results showed that TSA obtained a relatively higher amplification ratio, 7.6-fold (Fig. 4G and 4H), but it also introduced obvious nonspecific amplification, since strong fluorescence was observed in the cytoplasm (Fig. 4D). The nonspecific amplification of TSA increased 29% when the concentration of SA-HRP increased from 1:1000 to 1:300 (Fig. S7). Finally, the signal-to-noise ratio of Click-based amplification was 36.2, while that of TSA was only 4.8, mainly resulting from the high nonspecific binding of HRP.

HRP is a glycoprotein with nine potential N-glycosylation sites, and the carbohydrate content reaches about 20% (w/w).<sup>19</sup> The high glycosylation of HRP may mediate relatively high nonspecific binding and high background amplification.<sup>20</sup> On the contrary, streptavidin has no glycosylation, which helps to



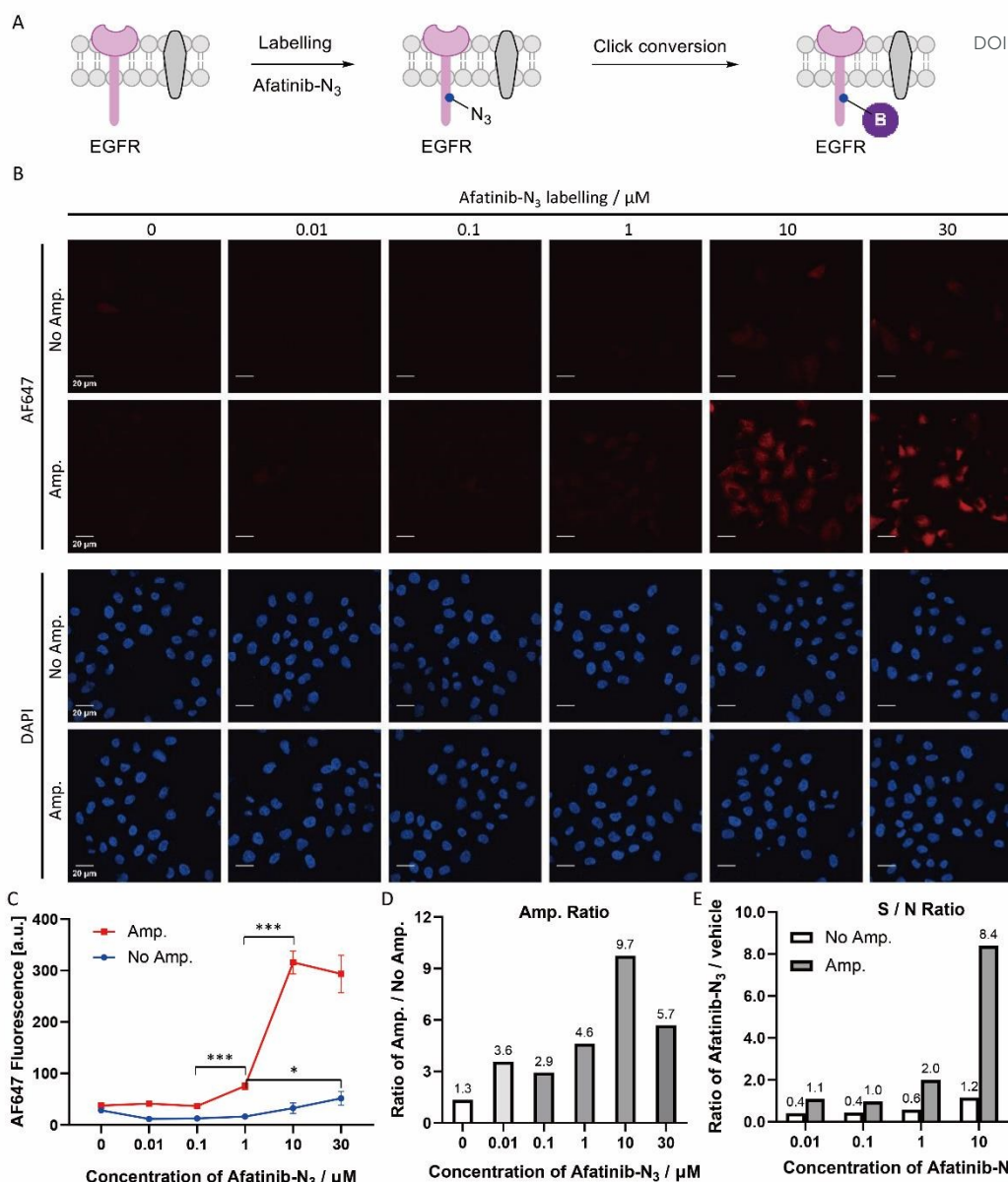


Fig. 5 Click-based amplification on fixed HeLa cells with Afatinib-N<sub>3</sub> labelling. (A) Scheme of Afatinib-N<sub>3</sub> labelling on EGFR protein and the click conversion of N<sub>3</sub> to biotin. (B) Confocal imaging of fixed HeLa cells without and with Click-based amplification (No Amp. and Amp.). HeLa cells were treated with a concentration gradient of Afatinib-N<sub>3</sub> from 0.01  $\mu\text{M}$  to 30  $\mu\text{M}$  in DMEM at 37  $^{\circ}\text{C}$  for 1 h. DAPI indicated the nucleus of the HeLa cell. Scale bar, 20  $\mu\text{m}$ . (C) Quantification of cellular AF647 fluorescence intensity in (B) with ImageJ. Red line represents the fluorescence intensity of HeLa cells with Click-based amplification (Amp.), and each data point is the average fluorescence intensity of 20 cells chosen randomly from the microscope imaging. Blue line, the fluorescence intensity of HeLa cells without Click-based amplification (No Amp.). Error bar: the standard error (SE). (D) Amplification ratios (Amp. / No Amp.). (E) Signal-to-noise ratios (Afatinib-N<sub>3</sub> / vehicle). \*\*\* =  $p < 0.001$ , \* =  $p < 0.05$ .

explain the ultralow background amplification of Click-based amplification.

#### Click-based amplification for covalent inhibitor probe mediated protein labelling in HeLa cells

Covalent inhibitors are compounds that designed to form a covalent bond with its specific molecular target. Today, there are more than 50 approved drugs that act as covalent inhibitors targeting kinases, RAS proteins, cathepsin, caspases and other enzymes.<sup>21, 22</sup> Afatinib is a covalent inhibitor of EGFR with an IC<sub>50</sub>

value of 0.5 nM, and was approved by the FDA and EMA in 2013 for the treatment of patients with advanced non-small cell lung cancer (NSCLC).<sup>23</sup> HeLa cell expresses high level of EGFR, and afatinib inhibits the growth of HeLa cell with an IC<sub>50</sub> value of 6.8  $\mu\text{M}$ .<sup>24</sup> We designed and synthesized an azide functionalized probe Afatinib-N<sub>3</sub> by replacing one N-methyl with a propyl azide group in our previous published paper.<sup>25</sup> HeLa cells were treated with a gradient of Afatinib-N<sub>3</sub> from 0.01  $\mu\text{M}$  to 30  $\mu\text{M}$  (Fig. 5B). In the amplification group (Fig. 5C, Amp.), HeLa cells treated with 1  $\mu\text{M}$  of Afatinib-N<sub>3</sub> began to show a significant fluorescence



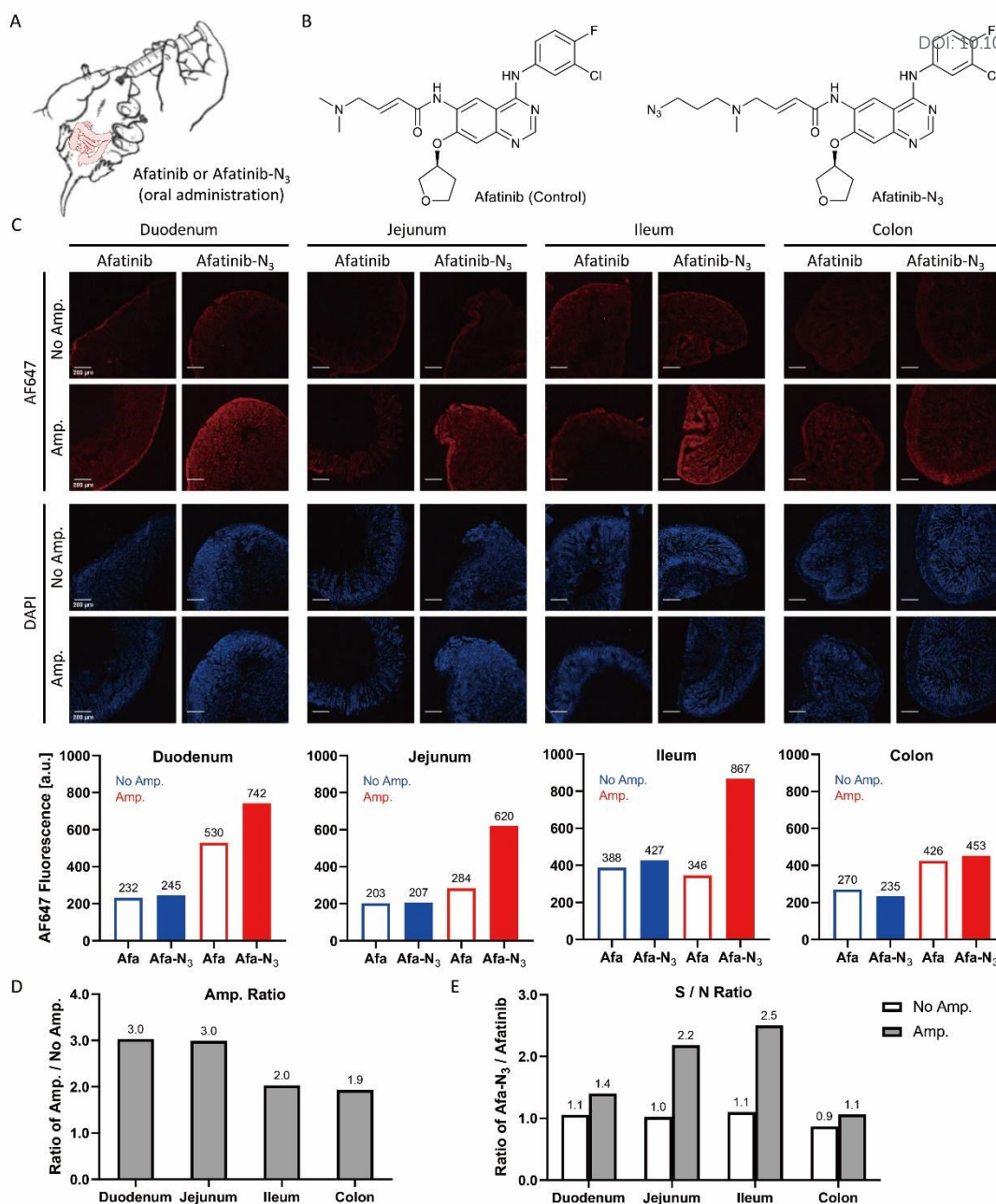


Fig. 6 Click-based amplification on fixed intestinal sections of mice treated with Afatinib-N<sub>3</sub>. (A) Scheme of mice P.O treatment with Afatinib and Afatinib-N<sub>3</sub>. (B) Structure of Afatinib (Control) and Afatinib-N<sub>3</sub>. (C) Up: confocal imaging of fixed intestinal sections without and with Click-based amplification. Mice were given oral administration of Afatinib (10.0 mg/kg) or Afatinib-N<sub>3</sub> (11.4 mg/kg, equal mol), and dissection was carried out 24 h later. DAPI indicated the nucleus of the intestinal cells. Scale bar, 200  $\mu$ m. Down: Quantification of tissue fluorescence intensity. Whole specimen was circled and measured the mean fluorescence intensity with ImageJ. Blue column, tissue fluorescence intensity without Click-based amplification. Red column, tissue fluorescence intensity with Click-based amplification. (D) Amplification ratios (Amp. / No Amp.). (E) Signal-to-noise ratios (Afatinib-N<sub>3</sub> / Afatinib).

increase, while in the group without amplification (Fig. 5C, No Amp.), HeLa cells treated with 30  $\mu$ M of Afatinib-N<sub>3</sub> began to show a labelling-dependent fluorescence increase. Click-based amplification therefore improved the detection sensitivity by at least 30-fold. In view of the IC<sub>50</sub> value of 6.8  $\mu$ M inhibiting HeLa cell growth, Click-based amplification offers a more suitable imaging tool to reveal the relationship between cellular location and biological function of small molecule inhibitors. Besides,

Click-based amplification obtained fluorescence amplification by 4.6-9.7 fold in fixed HeLa cells treated with 1-30  $\mu$ M of Afatinib-N<sub>3</sub> (Fig. 5D). The signal-to-noise ratios of cellular fluorescence were also improved by Click-based amplification (Fig. 5E).

#### Click-based amplification for drug distribution in mice intestinal sections





Afatinib frequently brings side effects for patients such as diarrhea, acneiform eruption, mouth sores, paronychia and dry mouth during clinical use.<sup>26, 27</sup> The signalling pathway modulations of afatinib have been uncovered,<sup>28, 29</sup> but there are currently few methods that can detect the localization of afatinib in tissues and provide direct evidences of the participation of afatinib in side effects occurrence. Y. Yamamoto et al developed an immunohistochemistry (IHC) protocol using a specific anti-afatinib antibody and HRP/DAB (3,3'-diaminobenzidine) staining system to detect afatinib-protein conjugates in fixed rat intestines and skin tissues.<sup>30</sup> Here, we treated mice with Afatinib-N<sub>3</sub> probe (Fig. 6A and 6B) and carried out Click-based amplification in fixed intestinal sections from duodenum, jejunum, ileum and colon. The fluorescence signals of sections from duodenum, jejunum and ileum were enhanced with Click-based amplification by 2-3 fold (Fig. 6C and 6D). The signal-to-noise ratios were also increased significantly with Click-based amplification for sections from jejunum and ileum (Fig. 6E). Sections from colon showed weakest fluorescence signals among these intestinal specimens, which suggested that the distribution of Afatinib-N<sub>3</sub> in colon was low. Taken together, Click-based amplification may serve as a useful tool to detect drug distribution in tissues.

## Conclusions

In summary, Click-based amplification has been demonstrated to amplify various click-labelling systems with ultralow background amplification. The streptavidin-based amplifier is a minimalist design: with a moderate number of functional groups, homogenous, of small size, cheap on market, and stored as ready-to-use aliquots in refrigerator. Picolyl azide (pAz) was used as the functional group of amplifier to accelerate the click conversion.

Click-based amplification could be well integrated with various click-labelling modes, and provided fluorescence amplification for NHS-N<sub>3</sub>, EdU and Afatinib-N<sub>3</sub> labelling by 3.0-12.7 fold in fixed HeLa cells. Compared with the widely used TSA, Click-based amplification introduced very low nonspecific amplification when used in cell imaging, and gave a higher signal-to-noise ratio. Signal amplification of tissue specimen is challenging. Click-based amplification achieved a moderate signal amplification and improved the signal-to-noise ratio of Afatinib-N<sub>3</sub> labelling in fixed mice intestinal sections. Tissue imaging with drug probe would provide direct visualization of drug distribution, and could be complementary to target protein imaging. Collectively, we could expect that this newly developed Click-based amplification method will find broad applications in biomedical research.

## Experimental Methods

### General organic synthesis

The organic reactions involved in this work were carried out in flasks containing argon atmosphere, which were sealed with rubber

stopper. All chemical reagents purchased from commercial suppliers were used without further purification. The reaction solvents were ultra-dry solvents containing molecular sieve, and transferred with injection syringes. TLC and LC-MS were used to monitor reactions, and silica gel column chromatography purifications were carried out to separate the intermediates and products. Products were characterized with <sup>1</sup>H-NMR (400 MHz), <sup>13</sup>C-NMR (101 MHz) and HRMS.

### Proteins and chemicals

Streptavidin (bs-0437P, Bioss), Streptavidin-AF647 (bs-0437P-AF647, Bioss), SA-HRP (B110053-0100, Diamond), Biotin-XX Tyramide (A8012-10, Apexbio), BCA Protein Assay Kit (PT0001, Leagene), Prolong Gold Antifade Mountant with DAPI (P36941, Invitrogen), EdU (ST067, Beyotime), Afatinib (BD210970, Bidepharm), Biotin-PEG<sub>4</sub>-alkyne (#764213, Sigma), BTAA (BDJ-4, Confluore).

### Streptavidin-based amplifiers synthesis

**Streptavidin-N<sub>3</sub>:** To a solution of streptavidin (2 mg/mL) in PBS, DMSO stock solution of NHS-N<sub>3</sub> was added in one portion and the final working concentration of NHS-N<sub>3</sub> was 6.9 mM (200 eq.). The reaction mixture was rolling over at room temperature for 2 h, then loaded to a HiTrap desalting column (29-0486-84, GE). Protein fractions were collected and combined. The concentration of streptavidin-N<sub>3</sub> was quantified with BCA Protein Assay Kit (streptavidin as the standard protein). The protein solution was divided into 10 μL aliquots and stored in -80 °C refrigerator as a ready-to-use reagent.

**Streptavidin-pAz:** To a solution of streptavidin (2 mg/mL) in PBS, DMSO stock solution of NHS-pAz was added in one portion and the final working concentration of NHS-pAz was 5.0 mM (145 eq.). The reaction mixture was rolling over at room temperature for 4 h, then loaded to a HiTrap desalting column. The following operations were same as streptavidin-N<sub>3</sub>.

### Click conversion of amplifiers in solution

To a solution of streptavidin-N<sub>3</sub> (0.21 mg/mL by BCA) or streptavidin-pAz (0.17 mg/mL by BCA) in PBS, 0.5 mM of biotin-PEG<sub>4</sub>-alkyne, 0.5 mM of CuSO<sub>4</sub>, 1 mM of BTAA and 2.5 mM of sodium ascorbate were added. The reaction mixture was rolling over at room temperature for 2 h, then another 2.5 mM of sodium ascorbate was added. The reaction was maintained for another 1 h. The protein product was purified with HiTrap desalting column, using Milli-Q purified water as the eluent. After freeze drying, the protein powder was redissolved with water containing 0.3% formic acid. The protein sample was analysed with ESI-TOF mass spectrometer. Molecular weight was obtained after deconvolution, and the click conversion efficiency was calculated based on the integration of MS peaks.

### Cell culture and labelling

**Cell culture:** HeLa cells were maintained in DMEM (Gibco) supplemented with 10% (v/v) fetal bovine serum (Gibco) and 100 IU of penicillin-streptomycin (Gibco) in a 37 °C incubator with 5% CO<sub>2</sub>. For click-labelling and fluorescence imaging, HeLa cells were resuspended at a concentration of 100,000 cells/mL in DMEM medium and seeded in a 24-well plate by 0.5 mL/well. A 12 mm glass coverslip was placed on the bottom of each well to allow HeLa cells adhesion.



**NHS-N<sub>3</sub> labelling and click conversion:** HeLa cells adhered to the glass coverslip in 24-well plate overnight. The medium was removed, and cells were washed with ice-cooled PBS twice, and then placed on ice. NHS-N<sub>3</sub> was diluted with ice-cooled PBS to a concentration gradient from 0.1 μM to 10 μM, and added into the 24-well plate. HeLa cells were treated with NHS-N<sub>3</sub> on ice for 30 min, and washed with PBS twice. Cell fixation with 4% PFA was carried out at room temperature for 10 min, and then quenched with 50 mM of NH<sub>4</sub>Cl/glycine in PBS. The click conversion of N<sub>3</sub> labelling was performed with 10 μM of biotin-PEG<sub>4</sub>-alkyne, 100 μM of CuSO<sub>4</sub>, 200 μM of BTAA and 2.5 mM of sodium ascorbate in PBS at room temperature for 30 min. Cells were washed with PBS five times after click reaction.

**EdU labeling and click conversion:** After adhesion to glass coverslip, HeLa cells were treated with 10 μM of EdU in DMEM medium overnight. The medium was removed, and cells were washed with PBS twice. Cell fixation with 4% PFA was carried out at room temperature for 10 min, and then quenched with 50 mM of NH<sub>4</sub>Cl/glycine in PBS. Cells were permeabilized with 0.2% Triton X-100 in PBS for 10 min, and washed with PBS twice. The click conversion of alkyne labelling was performed with 10 μM of biotin-N<sub>3</sub>, 100 μM of CuSO<sub>4</sub> and 2.5 mM of sodium ascorbate in PBS at room temperature for 30 min. BTAA was absent in the click reaction, because it slowed down the click conversion of EdU in HeLa cells (Fig. S6). Cells were washed with PBS five times after click reaction.

**Afatinib-N<sub>3</sub> labelling and click conversion:** HeLa cells adhered to glass coverslip on the bottom of 24-well plate overnight. A series of 500x DMSO stock solutions (1 μL) of Afatinib-N<sub>3</sub> were added to the cell culture medium directly and mixed well. The final working concentration gradient of Afatinib-N<sub>3</sub> was from 0.01 μM to 30 μM. HeLa cells were maintained in incubator for 1 h. Then the medium was removed, and cells were washed with PBS twice. Cell fixation and click conversion were carried out same as NHS-N<sub>3</sub> labelling.

#### Click-based amplification workflow

**Streptavidin-pAz binding:** To the HeLa cells containing biotin labelling, 0.5 μg/mL of streptavidin-pAz in PBS was added. The cells were maintained at room temperature for 40 min, then washed with PBS twice. The unoccupied biotin-binding pockets of streptavidin were blocked with 0.5 mM of biotin in PBS at room temperature for 5 min, and HeLa cells were washed with PBS twice.

**Click conversion:** The click conversion of pAz groups on target was performed with 10 μM of biotin-PEG<sub>4</sub>-alkyne, 100 μM of CuSO<sub>4</sub>, 200 μM of BTAA and 2.5 mM of sodium ascorbate in PBS at room temperature for 30 min. Cells were washed with PBS five times after click reaction.

**Streptavidin-AF647 binding:** To the HeLa cells containing biotin labelling, 1.0 μg/mL of streptavidin-AF647 in PBS was added. The cells were maintained at room temperature for 40 min, then washed with PBS five times.

**Anti-fade mounting:** Prolong Gold Antifade Mountant with DAPI (10 μL) was pipetted onto a microscope slide. The glass coverslip with HeLa cells was taken out from 24-well plate with fine-tipped tweezers and covered onto the antifade mountant droplet (the side with cells faced down). The sample was kept in shady at room temperature for 24 h for solidification.

#### Tyramide signal amplification (TSA) workflow

TSA was carried out as the indication of The TSA Plus Biotin Kit (PerkinElmer, NEL749A001KT). TNT wash buffer contains 0.1 M of Tris-HCl (pH 7.5), 0.15 M of NaCl and 0.05% Tween 20.

**SA-HRP binding:** The HeLa cells containing biotin labelling were blocked with TNB buffer (TNT buffer + 0.5% BSA) for 30 min. SA-HRP (1:1000) in TNB buffer was added to HeLa cells and incubated for 30 min. Cells were washed with TNT buffer three times. (BSA was used as the blocking reagent in TNB buffer, because the recommended blocking reagent FP1020 by PerkinElmer was not commercially available at that moment)

**TSA amplification:** HeLa cells were incubated with amplification working solution containing 1 μg/mL of Biotin-XX-Tyramide (BXXP) and 1 mM of H<sub>2</sub>O<sub>2</sub> in 0.1 M borate buffer (pH 8.5) for 10 min, and washed with TNT buffer three times.

**Streptavidin-AF647 binding:** The HeLa cells containing biotin labelling were blocked with TNB buffer for 20 min. 1.0 μg/mL of streptavidin-AF647 in TNB buffer was added to HeLa cells and incubated for 30 min. Cells were washed with TNT buffer three times.

**Anti-fade mounting** was same as Click-based amplification.

#### Animals and Afatinib / Afatinib-N<sub>3</sub> treatment

All animals in this study were bought from company (Charles River, China) and acclimated for one week before experimental application. All the animals were conducted in the barrier facility of laboratory animal center with 12 hours light and 12 hours dark, and all experiments were approved by the institutional animal use and care committee. Male C57BL/6 (8 weeks) were divided into two groups: Afatinib group (n = 3) and Afatinib-N<sub>3</sub> group (n = 3). Both compounds were dissolved in a solution containing 10% DMSO and 40% 2-hydroxypropyl-beta-cyclodextrin in water, and orally administered to mice (10.0 mg/kg and 11.4 mg/kg respectively). Dissection was performed 24 h later. Duodenum, jejunum, ileum and colon specimens were collected and embedded in optimal cutting temperature compound (OCT compound). Cryostat sectioning was carried out by cutting 8 μm thick sections in slicer at -20 °C. The intestinal tissue sections were frozen at -80 °C before use.

#### Click-based amplification of mice intestinal sections

An ImmEdge™ Pen (Vector Laboratories, H-4000) was used for drawing a water-repellent barrier around tissue section that was mounted on microscope slide. The tissue specimen was washed with PBS twice, fixed with 4% PFA for 10 min, and then quenched with 50 mM of NH<sub>4</sub>Cl/glycine in PBS. The click conversion of N<sub>3</sub> labelling was performed with 10 μM of biotin-PEG<sub>4</sub>-alkyne, 100 μM of CuSO<sub>4</sub>, 200 μM of BTAA and 2.5 mM of sodium ascorbate in PBS at room temperature for 30 min. The tissue specimen was washed with PBS five times after click reaction.

The Click-based amplification workflow for fixed tissue section was same as mentioned above except the anti-fade mounting. Prolong Gold Antifade Mountant with DAPI (10 μL) was pipetted onto the tissue specimen directly, and then an 18 mm x 18 mm glass coverslip was covered onto the tissue specimen. The sample was kept in shady at room temperature for 24 h for solidification.

#### Confocal imaging and fluorescence quantification

**Confocal imaging method:** Cells on 12 mm coverslips were imaged using an inverted TiE A1 confocal microscope (Nikon) equipped with a 60x/1.40 NA oil-immersion objective, a 405 nm blue-violet laser



(Coherent) and a 641 nm laser (Coherent). Blue and red fluorescence were collected using a 450/50 nm emission filter and a 700/75 nm emission filter, respectively. Tissue sections were imaged using the same confocal microscope but equipped with a 10×/0.45 NA objective.

**Cellular fluorescence quantification with ImageJ:** Single cell was circled along the membrane edge and measured the mean fluorescence intensity, a similar field without any cells was circled and measured as the background fluorescence, and the difference was defined as cellular fluorescence intensity. Generally, 20 cells were chosen randomly and averaged to get the mean cellular fluorescence and the SE value, and an example was given in Fig. S4. For HeLa cells with EdU labelling, all the lighted nucleuses were circled and measured to calculate the average nucleus fluorescence intensity.

## Ethical Statement

All animal procedures were performed in accordance with the Guidelines for Care and Use of Laboratory Animals of Peking University and approved by the Animal Ethics Committee of Peking University.

## Author Contributions

X. Lei and Y. Li conceived the project. J. Bai performed the organic synthesis, protein modification, cell labelling and amplification, confocal imaging and fluorescence quantification. F. Guo performed the mice treatment, the surgery and mice intestinal freeze section preparation. M. Li participated in early-stage setup and experiment design. All authors contributed to the data processing and analysis. J. Bai and X. Lei wrote the manuscript with input from other authors.

## Conflicts of interest

There are no conflicts to declare.

## Acknowledgements

This project was supported by National Key Research & Development Plan (2017YFA0505200 to Xiaoguang Lei), the National Natural Science Foundation of China Grant (21625201, 21961142010, 21661140001, 91853202 and 21521003 to Xiaoguang Lei), the Beijing Outstanding Young Scientist Program (BJJWZYJH01201910001001 to Xiaoguang Lei) and the Beijing Brain Initiative of the Beijing Municipal Science & Technology Commission (Z181100001518004 to Yulong Li) is gratefully acknowledged.

## References

1. M. N. Bobrow, T. D. Harris, K. J. Shaughnessy and G. J. Litt, *J Immunol Methods*, 1989, **125**, 279-285.
2. R. M. Dirks and N. A. Pierce, *Proceedings of the National Academy of Sciences of the United States of America*, 2004, **101**, 15275.

3. R. Lin, Q. Feng, P. Li, P. Zhou, R. Wang, Z. Liu, Z. Wang, X. Qi, N. Tang, F. Shao and M. Luo, *Nat Methods*, 2018, **15**, 275-278.
4. S. K. Saka, Y. Wang, J. Y. Kishi, A. Zhu, Y. Zeng, W. Xie, K. Kirli, C. Yapp, M. Cicconet, B. J. Beliveau, S. W. Lapan, S. Yin, M. Lin, E. S. Boyden, P. S. Kaeser, G. Pihan, G. M. Church and P. Yin, *Nature Biotechnology*, 2019, **37**, 1080-1090.
5. M. Beck, A. Schmidt, J. Malmstroem, M. Claassen, A. Ori, A. Szymborska, F. Herzog, O. Rinner, J. Ellenberg and R. Aebersold, *Mol Syst Biol*, 2011, **7**, 549-549.
6. S. H. Rouhanifard, I. A. Mellis, M. Dunagin, S. Bayatpour, C. L. Jiang, I. Dardani, O. Symmons, B. Emert, E. Torre, A. Cote, A. Sullivan, J. A. Stamatoyannopoulos and A. Raj, *Nature Biotechnology*, 2019, **37**, 84-89.
7. Y. Cho, J. Seo, Y. Sim, J. Chung, C. E. Park, C. G. Park, D. Kim and J. B. Chang, *Nanoscale*, 2020, **12**, 23506-23513.
8. S. Tommasone, F. Allabush, Y. K. Tagger, J. Norman, M. Köpf, J. H. R. Tucker and P. M. Mendes, *Chemical Society Reviews*, 2019, **48**, 5488-5505.
9. L. K. Mahal, K. J. Yarema and C. R. Bertozzi, *Science*, 1997, **276**, 1125.
10. A. Salic and T. J. Mitchison, *Proceedings of the National Academy of Sciences*, 2008, **105**, 2415.
11. L. Wang, J. Xie and P. G. Schultz, *Annual Review of Biophysics and Biomolecular Structure*, 2006, **35**, 225-249.
12. N. Raddaoui, S. Stazzoni, L. Möckl, B. Viverge, F. Geiger, H. Engelke, C. Bräuchle and T. A.-O. Carell, *Chembiochem*, 2017, **18**, 1716-20.
13. I. Le Trong, Z. Wang, D. E. Hyre, T. P. Lybrand, P. S. Stayton and R. E. Stenkamp, *Acta crystallographica. Section D, Biological crystallography*, 2011, **67**, 813-821.
14. H. Kolb, M. Prof and K. Prof, *Angewandte Chemie*, 2001, **113**, 2056-2075.
15. N. J. Agard, J. M. Baskin, J. A. Prescher, A. Lo and C. R. Bertozzi, *ACS Chemical Biology*, 2006, **1**, 644-648.
16. R. van Geel, G. J. Pruijn, F. L. van Delft and W. C. Boelens, *Bioconjug Chem*, 2012, **23**, 392-398.
17. G.-C. Kuang, H. A. Michaels, J. T. Simmons, R. J. Clark and L. Zhu, *The Journal of Organic Chemistry*, 2010, **75**, 6540-6548.
18. C. Uttamapinant, A. Tangpeerachaikul, S. Grecian, S. Clarke, U. Singh, P. Slade, K. R. Gee and A. Y. Ting, *Angewandte Chemie International Edition*, 2012, **51**, 5852-5856.
19. M. Wuhler, C. I. A. Balog, C. A. M. Koeleman, A. M. Deelder and C. H. Hokke, *Biochimica et Biophysica Acta (BBA) - General Subjects*, 2005, **1723**, 229-239.
20. D. W. Ralin, S. C. Dultz, J. E. Silver, J. C. Travis, M. Kullolli, W. S. Hancock and M. Hincapie, *Clinical Proteomics*, 2008, **4**, 37-46.
21. F. Sutanto, M. Konstantinidou and A. Dömling, *RSC Medicinal Chemistry*, 2020, **11**, 876-884.
22. A. K. Ghosh, I. Samanta, A. Mondal and W. R. Liu, *ChemMedChem*, 2019, **14**, 889-906.
23. R. T. Dungo and G. M. Keating, *Drugs*, 2013, **73**, 1503-1515.
24. Y. Tu, Y. OuYang, S. Xu, Y. Zhu, G. Li, C. Sun, P. Zheng and W. Zhu, *Bioorg Med Chem*, 2016, **24**, 1495-1503.
25. D. E. Sun, X. Fan, Y. Shi, H. Zhang, Z. Huang, B. Cheng, Q. Tang, W. Li, Y. Zhu, J. Bai, W. Liu, Y. Li, X. Wang, X. Lei and X. Chen, *Nat Methods*, 2020, DOI: 10.1038/s41592-020-01005-2.
26. K. Park, E. H. Tan, K. O'Byrne, L. Zhang, M. Boyer, T. Mok, V. Hirsh, J. C. Yang, K. H. Lee, S. Lu, Y. Shi, S. W. Kim, J. Laskin, D. W. Kim, C. D. Arvis, K. Kölbeck, S. A. Laurie, C. M. Tsai, M. Shahidi, M. Kim, D. Massey, V. Zazulina and L. Paz-Ares, *The Lancet. Oncology*, 2016, **17**, 577-589.



27. J. C. Soria, E. Felip, M. Cobo, S. Lu, K. Syrigos, K. H. Lee, E. Göker, V. Georgoulas, W. Li, D. Isla, S. Z. Guclu, A. Morabito, Y. J. Min, A. Ardizoni, S. M. Gadgeel, B. Wang, V. K. Chand and G. D. Goss, *The Lancet. Oncology*, 2015, **16**, 897-907.
28. Y.-C. Tsai, C.-H. Yeh, K.-Y. Tzen, P.-Y. Ho, T.-F. Tuan, Y.-S. Pu, A.-L. Cheng and J. C.-H. Cheng, *European Journal of Cancer*, 2013, **49**, 1458-1466.
29. Y. Chen, X. Chen, X. Ding and Y. Wang, *Molecular medicine reports*, 2019, **20**, 3317-3325.
30. Y. Yamamoto, T. Saita, Y. Yamamoto, R. Sogawa, S. Kimura, Y. Narisawa, S. Kimura and M. Shin, *Acta Histochem*, 2019, **121**, 151439.

View Article Online  
DOI: 10.1039/D1CB00002K

Open Access Article. Published on 20 March 2021. Downloaded on 3/21/2021 9:03:21 AM.  
This article is licensed under a Creative Commons Attribution 3.0 Unported Licence.

